HHS Public Access

Author manuscript

Nature. Author manuscript; available in PMC 2020 June 04.

Published in final edited form as:

Nature. 2020 January ; 577(7788): 85–88. doi:10.1038/s41586-019-1819-6.

RGF1 controls root meristem size through ROS signaling

Masashi Yamada[1,2,3], **Xinwei Han**[1,4], **Philip N. Benfey**[1,*]

[1]Department of Biology and HHMI, Duke University, Durham, NC 27710, U.S.A.

[2]Agricultural Biotechnology Research Center, Academia Sinica, Taipei 115, Taiwan

[3]Biotechnology Center in Southern Taiwan, Academia Sinica, Tainan 741, Taiwan

Abstract

Stem cell niche and root meristem size are maintained by intercellular interactions and signaling networks of a peptide hormone, Root Meristem Growth Factor 1 (RGF1). How RGF1 regulates root meristem development is an essential question to understand stem cell function. Although five receptors of RGF1 have been identified, the downstream signaling mechanism remains unknown. Here, we report a series of signaling events following RGF1 action. The RGF1-receptor pathway controls the distribution of reactive oxygen species (ROS) along the developmental zones of the *Arabidopsis* root. We identify a novel transcription factor, *RGF1 INDUCIBLE TRANSCRIPTION FACTOR 1* (*RITF1*) that plays a central role in mediating RGF1 signaling. Manipulating *RITF1* expression leads to redistribution of ROS along the root developmental zones. Changes in ROS distribution, in turn, enhance the stability of the PLETHORA2 (PLT2) protein, a master regulator of root stem cells. Our study, thus, clearly depicts a signaling cascade initiated by RGF1, linking the RGF1 peptide to ROS regulatory mechanisms.

Roots encounter various environmental conditions and respond by altering their growth. Root growth arises through controlled cell division in the meristematic zone, equivalent to the transit amplifying zone in animals. After division, most cells increase their size in the elongation zone and mature in the differentiation zone. The size of these developmental zones is determined by intrinsic and extrinsic signals. Reactive oxygen species (ROS) are an intrinsic signal for establishing the size of the meristematic zone. Superoxide (O_2^-) primarily accumulates in the meristematic zone, while hydrogen peroxide (H_2O_2) mainly accumulates in the differentiation zone[1,2]. The balance between O_2^- and H_2O_2 modulates the transition from proliferation to differentiation[2].

---

*Correspondence and requests for materials should be addressed to P.N.B. (philip.benfey@duke.edu).

Author contributions:

M.Y. and P.N.B. conceptualized the study; M.Y. performed all experiments; X.H. performed the computational analyses; all authors wrote the paper.

[4]Current address: GlaxoSmithKline, 1000 Winter St, Waltham, MA 02451. U.S.A.

Supplementary Information is available in the online version of the paper.

The authors declare no competing interests: details are available in the online version of the paper. Readers are welcome to comment on the online version of the paper.

A previous version of this work was deposited in the pre-print depository server bioRxiv. doi: https://doi.org/10.1101/244947

The RGF1 peptide is an essential hormone in controlling the size of the meristematic zone both as an intrinsic and extrinsic signal [3-5]. RGF1 treatment increases the size of the meristematic zone, while the *rgf1/2/3* triple mutant has a smaller meristematic zone[3]. Quintuple mutants of the *rgf1 receptor* (*rgfr*) lack most cells in the root meristem and are insensitive to RGF1[6-8]. RGF1 signaling controls the stability of the PLETHORA (PLT) 1/2 proteins[3], which are required for stem cell maintenance[9]. However, it is not known how RGF1 modulates the size of the meristematic zone and the stability of PLT1/2.

After RGF1 treatment, the meristematic zone-specific marker HIGH PLOIDY2 (HPY2)-GFP[10] was detected in an enlarged area, correlating with a larger meristematic zone (Extended Data Fig. 1a-c), suggesting RGF1 controls gene expression primarily in the meristematic zone. Therefore, to identify target genes downstream of RGF1, we isolated the meristematic zone one hour after RGF1 treatment (Extended Data Fig. 1d). Since *HPY2-GFP* expression and the meristematic zone size were unchanged in this time period, we can exclude the possibility that an enlarged meristem is the reason for changes in RNA levels. RNA-seq profiling found 583 differentially expressed genes between RGF1 and mock treatment (Supplementary Table 1). Gene Ontology highly enriched categories included “glutathione transferase activity” and “oxidoreductase activity” (Extended Data Fig. 2 and Supplementary Table 2), suggesting RGF1 might signal through an ROS intermediate.

To examine the relationship between RGF1 and ROS signaling, we analyzed the distribution of O_2^- and H_2O_2 after RGF1 treatment. The specific indicator for H_2O_2, H_2O_2-3’-O-Acetyl-6’-O-pentafluorobenzenesulfonyl-2’-7’-difluorofluorescein-Ac (H_2O_2-BES-Ac)[2], exhibited lower fluorescence in the meristematic and elongation zones 24 h after RGF1 treatment (Fig. 1a and c). O_2^- signals were detected by nitro blue tetrazolium (NBT) staining[1] and were observed more broadly in the meristematic zone 24 h after RGF1 treatment (Fig. 1b and d). In the RGF1 receptor mutant *rgfr1/2/3*, whose meristematic zone is unchanged after RGF1 treatment (Fig.1e), levels of H_2O_2 and O_2^- were comparable between mock and RGF1 treatments (Fig. 1e-h).

To identify downstream factors in the RGF1/ROS signaling pathway, we combined our RGF1 transcriptome data with developmental zone-specific transcriptome data[11]. Among genes that are both meristematic zone-specific and induced by RGF1, we identified the *PLANT AT-RICH SEQUENCE and ZINC-BINDING TRANSCRIPTION FACTOR* (*PLATZ*) *FAMILY PROTEIN* gene (AT2G12646) whose expression increased approximately 2-fold after 1 hour of RGF1 treatment (Fig. 2a). We named this gene, *RGF1 INDUCIBLE TRANSCRIPTION FACTOR* 1 (*RITF1*), and found that its expression is predominantly in the meristematic zone[11] (Fig. 2b). Quantitative RT-PCR showed *RITF1* transcript abundance increased approximate 2-fold in wild type one hour after RGF1 treatment, and was maintained at 6 and 24 hours (Fig. 2c). By contrast, *RITF1* expression in *rgfr1/2/3* was unchanged upon RGF1 treatment (Fig. 2c). Expression of a construct with the *RITF1* promoter driving the *GFP* coding sequence (*pRITF1-GFP*) mirrored our transcriptome analysis and increased in wild type following RGF1 treatment (Fig. 2b, d, and e). By contrast, *pRITF1-GFP* expression was very low and exhibited no change following RGF1 treatment in *rgfr1/2/3* (Fig. 2d and e). These data indicate that *RITF1* expression is regulated by the RGF1 pathway.

To understand its function, *RITF1* was inducibly overexpressed using the estradiol inducible promoter system[12]. After 24 h of β-estradiol treatment, the meristematic zone became enlarged and the number of cells increased (Fig. 2f and i) similar to that of RGF1 treated roots (Fig. 1a). We also found that H_2O_2 levels declined in all three developmental zones upon estradiol treatment (Fig. 2g and j) and enhanced O_2^- signals were observed in a broader area of the meristematic zone (Fig. 2h and k) with ectopic O_2^- signals in the elongation and differentiation zones (Fig. 2h). Altered ROS signals and an enlarged meristem suggest that *RITF1* can modulate ROS signaling and root meristem size downstream of the RGF1 pathway. We also observed an earlier response to induction of *RITF1* than to RGF1 treatment. A decrease in the BES-H_2O_2-Ac signal was detected 4 h after estradiol treatment (Extended Data Fig. 3a and b) as compared to no detectable change 4 h after RGF1 treatment in either the uninduced line or in wild type (Extended Data Fig. 3a and b). Changes in ROS signals were first observed at approximately 6 h after RGF1 treatment in those lines (Extended Data Fig. 4i, j, o, p, 5b, and c). If *RITF1* functions downstream of the RGF1-receptor pathway, overexpression of *RITF1* in *rgfr1/2/3* should rescue root meristem defects and increase root meristem size. To test this hypothesis, we inducibly overexpressed *RITF1* in *rgfr1/2/3* and in wild type and observed an enhanced O_2^- signal and increased root meristem size in both (Fig. 3a-d). Finally, we examined two *ritf1* mutant alleles. The *ritf1-1* allele was generated using CRISPR/Cas9 and contains a frameshift mutation early in the coding sequence, rendering it unlikely to produce a functional RITF1 protein. The *ritf1-2* allele has a T-DNA insertion in the intron, but still has low expression of full length *RITF1* and is likely to produce low levels of a functional protein. The *ritf1-1* mutant had a smaller meristem and lower root growth rate (Extended Data Fig. 6a and b) and was more resistant to RGF1 treatment than wild type or the weak allele, *ritf1-2* (Extended Data Fig. 6b and c). Further, there was lower induction of the O_2^- signal in *ritf1-1* after RGF1 treatment than wild type or *ritf1-2* (Fig. 3e and f). Taken together, these results strongly suggest that *RITF1* is a primary regulator of ROS signaling and root meristem size in the RGF1 signaling pathway.

To confirm post-translational regulation of PLT2, we compared transcriptional (*pPLT2-CFP*)[13] and translational (*gPLT2-YFP*)[13] fusion lines. At 24 h after RGF1 treatment, we observed broader localization of *gPLT2-YFP* (Extended Data Fig. 7b), while the localization and expression of *pPLT2-CFP* were comparable between Mock and RGF1 treatments, even though RGF1-treated roots had a larger meristematic zone (Extended Data Fig. 7a). The *gPLT2-YFP* signal decreased more gradually and was broadly localized in the larger meristematic zone after RGF1 treatment (Extended Data Fig. 7a-c). These results confirm that RGF1 regulates PLT2 post-translationally. *PLT2* is a member of the *APETALA2 / ETHYLENE RESPONSE FACTOR* transcription factor family, which is reported to be regulated by oxidative post-translational modification[14-19]. To determine if modifying the oxidative conditions can increase the stability of the PLT2 protein, we treated the *gPLT2-YFP* line with RGF1 and potassium iodide (KI), an H_2O_2 scavenger. We found that *gPLT2-YFP* was localized more broadly and meristem size increased compared to roots treated only with RGF1 (Fig. 4a-c). By contrast, increased H_2O_2 inhibited broad localization of *gPLT2-YFP* and reduced the increase of meristem size upon addition of RGF1 (Extended Data Fig. 8a-e). To decrease O_2^- levels, we used 500 nM diphenyleneiodonium (DPI), an NADPH

oxidase inhibitor (Fig. 4d-f), resulting in slight inhibition of PLT2 stability and meristem size (Fig. 4d-f) with little effect on root meristem development. However, co-treatment of RGF1 and DPI dramatically reduced PLT2 stability and meristem size as compared to RGF1 treatment alone (Fig. 4d-f). Finally, we measured *gPLT2-YFP*, O_2^-, and H_2O_2 in a time course (4-10 h) after RGF1 treatment. Broader localization of *gPLT2-YFP* and increased superoxide levels along with lower H_2O_2 signals at the distal end of the meristematic zone appeared 6h after treatment (Extended Data Fig. 4a-d, and 5a; 4i and j; 4o and p). At 8 and 10 h after treatment, expanded *gPLT2-YFP* expression and O_2^- signals correlated with declining H_2O_2 signals (Extended Data Fig. 4e-h, 4k-n, 4q-t, 5a-c). Taken together, these results indicate that ROS regulates PLT2 protein stability by modulating O_2^- and H_2O_2 levels.

To further test the hypothesis that PLT2 protein stability is enhanced by ROS signaling produced by *RITF1*, we overexpressed *RITF1* in the *plt2* mutant. This produced an increase in the O_2^- signal (Extended Data Fig. 9a and b) but was unable to induce an increase in root meristem size (Extended Data Fig . 9c and d). Furthermore, we detected only a subtle change in root meristem size in *plt2* as compared to wild type upon RGF1 treatment (Extended Data Fig. 10a and b). However, an elevated O_2^- signal was observed (Extended Data Fig. 10c and d). These results strongly suggest that ROS signals modulated by *RITF1* enhance PLT2 stability. In summary, we identified a novel transcription factor, *RITF1*, induced by RGF1 in the meristematic zone. This factor controls ROS levels, which in turn, regulate PLT2 protein stability and meristem size. Overall, our data demonstrate a key role for the peptide hormone, RGF1, in regulating root growth via modulation of ROS levels, which control the transition from proliferation to differentiation.

Methods:

Plant materials and growth conditions

All *Arabidopsis* mutants and marker lines used in this research are in the Columbia-0 (Col-0) background. The T-DNA insertion line of *plt2* (SALK_130119.20.25) was obtained from the Arabidopsis Biological Resource Center at Ohio State University. The T-DNA insertion was identified at 166 bp upstream of the transcription start site in the *plt2* mutant. Seeds were surface sterilized using 50 % (vol/vol) bleach and 0.1% Tween 20 (Sigma) for 15 min and then rinsed five times with sterile water. All seeds were plated on standard MS media (1× Murashige and Skoog salt mixture, Caisson Laboratories), 0.5 g/L MES, 1% Sucrose, and 1% Agar (Difco) and adjusted to pH 5.7 with KOH. All plated seeds were stratified at 4 °C for 2 d before germination. Seedlings were grown on vertically positioned square plates in a Percival incubator with 16 h of daily illumination at 22 °C.

The *ritf1* mutants

The *ritf1-1* mutant was generated using the egg cell-specific controlled CRISPR/Cas9 system[20].

SgRNA sequences are as followed:

RITF1-sgRNA1: GGGATGTCCATACCATGAGA CGG

RITF1-sgRNA2: CCGTCTACCACAGTTGATCG AGG

RITF1-sgRNA3: GGCGAACTTGAAGGAGTCTA TGG

RITF1-sgRNA4: GACTTTCAGTTGAGTCCTCA TGG

The CRISPR construct was transformed into Col using the Agrobacterium-mediated floral dip method. The mutant was identified by direct sequencing of PCR products of the targets in the offspring in T1, 2, and 3 generations. The loss-of-function *ritf1-1* allele contains an insertion of a cytosine at 74 bp after the transcription start site in the *RITF1* gene (771 bp). The additional insertion of a cytosine results in a frameshift and creates many premature stop codons after the insertion. To exclude issues related to off-target mutations, the sequences of three potential off-target genes (At5g25170, At1g70110, At3g20640) including similar sequences of the target sites were confirmed by direct sequencing of PCR products in the offspring in the T1, 2, and 3 generations. We didn't find any mutations in these genes. Further, we identified another independent CRISPR allele (*ritf1-3*). This allele contains an insertion of an adenine at 75 bp after the transcription start site in the *RITF1* gene. The additional insertion of an adenine results in a frameshift and creates many premature stop codons after the insertion. Similar to *ritf1-1*, seedlings from *ritf1-3* exhibited strong resistance to RGF1 peptide and didn't increase O_2^- levels as compared to wild type or to the weak allele (*ritf1-2*) (Extended Data Fig. 6d and e). These results can exclude the possibility that off-target mutations cause the RGF1-resistant phenotype. In the *ritf1-2* allele (SALK_081503C), the T-DNA insertion was identified at 787 bp downstream of the transcription start site (in the middle of the second intron) of the *RITF1* gene. Even though the insertion disrupted an intron, a full-length transcript was weakly detected in this allele.

Detecting *gPLT2-YFP* and ROS signals

The seedlings of wild type and the *rgfr1/2/3* mutant were grown for seven days on MS agar plates, then transferred to MS agar plates containing either water (mock) or 20 nM synthetic sulfated RGF1 peptide (Invitrogen). After RGF1 treatment, seedlings were stained for 2 min in a solution of 200 μM NBT in 20 mM phosphate buffer (pH 6.1) in the dark and rinsed twice with distilled water. For detection of hydrogen peroxide with BES-H_2O_2-Ac[21], seedlings were incubated in 50 μM BES-H_2O_2-Ac (WAKO) for 30 min in the dark, then mounted in 10 mg/mL propidium iodide (PI) in water[2]. Roots were observed using a 20 X objective with a Zeiss LSM 880 laser scanning confocal microscope. Excitation and detection windows were set as follows: BES-H_2O_2-Ac, excitation at 488nm and detection at 500-550 nm; PI staining, excitation at 561 nm and detection at 570-650 nm. Confocal images were processed, stitched, and analyzed using the Fiji package of ImageJ[22]. Maximum projection images were generated from about 30 z-section images of BES-H_2O_2-Ac staining. The average intensity of BES-H_2O_2-Ac in the meristematic zone was measured in 5 or 6 roots with three biological replicates. Images for NBT staining were obtained using a 10 X objective with a Leica DM 5000-B light microscope. The total intensities of NBT staining in the meristematic zone were measured in 10 roots with three biological replicates using the Fiji software package[22].

For shorter time course experiments, seedlings of *gPLT2-YFP*[13] were grown on MS agar plates for 7 days, then transferred to MS agar plates containing either water (mock) or 100 nM RGF1 peptide. At 4, 6, 8, and 10 h after transfer to RGF1 plates, images were taken with a confocal or light microscope after PI, NBT, and BES-H_2O_2-Ac staining, as described above.

Total RNA preparation, RNA amplification and library preparation for RNA-seq

The *HYP2-GFP*[10] line was grown on MS plates for 7 days. *HYP2-GFP* seedlings were then transferred into liquid MS media and treated with water (mock) or 100 nM RGF1 peptide in 6-well-plates for 1 h. After treatment with mock or RGF1, the seedlings were taken out of liquid MS media and transferred onto a 2 % agarose plate. Using an ophthalmic scalpel (Feather), the meristematic zone of the seedlings was precisely dissected based on *HYP2-GFP* fluorescence as detected under a dissecting microscope (Axio Zoom, Zeiss). Total RNA was extracted from 20 root sections treated with mock or 100 nM RGF1 using the RNeasy Micro Kit (Qiagen). For each treatment, three replicates of the RNA extractions were performed. All total RNA samples were treated with DNase I during RNA extraction. RNA quality was examined using a 2100 Bioanalyzer (Agilent). The RNA Integrity Number (RIN) was over 9.0 in all samples. The concentration of total RNA was measured by a Qubit (Invitrogen) instrument. For each replicate, 50 ng total RNA was amplified using the Ovation RNA-seq System V2 (NuGEN). Following amplification, 3 μg of cDNA was fragmented using the Covaris S-Series System. 400 ng of the fragmented cDNA with an average size of 400 bp was used for library preparation using the Ovation Ultralow System V2 (NuGEN). Illumina sequencing was performed at the Duke Genome Sequencing Shared Resource. The libraries for three biological replicates of mock and RGF1 treated meristematic zones were sequenced on an Illumina HiSeq 2000 (100 base paired end reads).

Differential expression analysis following RGF1 peptide treatment

Illumina sequencing reads were mapped to the TAIR10 Arabidopsis genome using Tophat V2.1.1. The parameters used for mapping were: “-N 5 --read-gap-length 5 --read-edit-dist 5 --b2-sensitive -r 100 --mate-std-dev 150 -p 5 -i 5 -I 15000 --min-segment-intron 5 --max-segment-intron 15000 --library-type fr-unstranded”. To select properly mapped reads with unique mapping positions, only alignments with flag of 83, 99, 147 or 163 and a mapping quality score of 50 were kept for further analysis. Mapping positions of these reads were compared with the Araport11 genome annotation (https://www.araport.org/downloads/Araport11_Release_201606/annotation) using HTseq-count (v0.6.1) with parameters “--stranded=no --mode=intersection-nonempty”, which generated read count per gene. The raw read counts of miRNA, lncRNA and protein coding genes were then used as input into DESeq2 (v1.14.1) for differential gene expression analysis. Genes with an FDR-adjusted p-value less than or equal to 0.1 were regarded as differentially expressed between RGF treatment and mock. The enriched gene ontology (GO) groups among differentially expressed genes were identified using agriGO. The GO annotation downloaded from http://geneontology.org was used as input for agriGO. Enriched GO groups required an FDR-adjusted p-value of 0.01 or less and a minimum mapping entry of 10.

Expression analysis of *RITF1* upon RGF1 treatment by qRT-PCR

To perform qRT-PCR, about 20 meristematic zones of wild type and the *rgfr1/2/3* mutant were dissected at 1, 6, and 24h after RGF1 treatment as described above. cDNA was generated from ten micrograms of total RNA using SuperScript IV Reverse Transcriptase (Invitrogen). Three biological replicates and technical replicates were used for each experiment. Standard curves were run for the primer pairs of *RITF1* 5'-CAAGCCATGCCACACTCTAA-3' and 5'- TTATCCGAGGAAGCTGAGGA-3', and *PROTEIN PHOSPHATASE 2A SUBUNIT A3* (*PP2AA3*, AT1G13320) as reference 5'-GGCCAAAATGATGCAATCTC-3' and 5'- TGCGAAATACCGAACATCAA-3'. Expression of *RITF1* was assayed by qRT-PCR on a LightCycler 480 (Roche) with SYBR-based detection, normalized to *PP2AA3*, and analyzed by the efficiency corrected quantification (ECQ) model.

Plasmid Constructs

The coding sequence and the promoter sequence (2121 bp) of the *RITF1* gene (AT2G12646) were amplified using the Phusion High-Fidelity DNA polymerase (New England Biolabs) from a wild-type cDNA library and genomic DNA, respectively, then sub-cloned into the *pENTR/D/TOPO* vector (Invitrogen). The following primers were used for *RITF1* amplification: 5'-CACCATGGGAATTCAGAAACCGG-3' and 5'-TTAACAGAGAGGAGATCGTTG-3' and *RITF1* promoter amplification 5'-CACCGCATCATTTTATTATAACCCGA-3' and 5'-GAGGACTCAACTGAAAGTCA-3'. The sequence of the *RITF1* gene and the *RITF1* promoter in *pENTR/D/TOPO* vector was confirmed by Sanger sequencing. The clones were recombined into the *pMDC7* and *pMDC204* vectors[12] using LR clonase II (Invitrogen) to fuse the estradiol inducible promoter (*XVE*)[23] and the coding region of the *RITF1* gene and the *RITF1* promoter and GFP with a C-terminus HDEL retention sequence.

Measurement of meristem size and detection of ROS signals after overexpression of *RITF1*

The *XVE-RITF1* construct was transformed into wild type (Col). To measure meristem size and detect ROS signals, two independent lines of *XVE-RITF1* and wild type were grown on MS media for seven days, then transferred to MS media containing DMSO (Mock) and 10 μM β-estradiol (Sigma). After 24 h with mock or estradiol treatment, meristem size and ROS signals were measured and detected in wild type and the *XVE-RITF1* lines, as described above.

Expression of *pRITF1-GFP* in roots

The *pRITF1-GFP* construct was introduced into wild type (Col) and *rgfr1/2/3*. Two independent T3 lines in each background were grown for 7 days in MS media were treated with mock and 20 nM RGF1 peptide. 24 h after treatment, GFP signals were detected using a confocal laser scanning microscope, as described above.

Note:

***UPB1* is not required for the RGF1-receptor pathway—**We have previously reported that UPBEAT1 (UPB1) reduces H_2O_2 levels and controls meristem size by down-

regulating peroxidase genes in the elongation zone[2]. Our transcriptome analysis didn't find significant changes in *UPB1* expression upon RGF1 treatment (Supplementary Table 1 and 3). We did find elevated expression of 5 peroxidase genes (Supplementary Table 1), but these are not targets of *UPB1*[2], suggesting that RGF1 regulates meristem size independently of *UPB1*. To determine if the peroxidase genes upregulated by RGF1 play a role in meristem size control in the RGF1-signaling pathway, we overexpressed two of them (At5g39580 and At4g08780). In neither case did we observe a larger meristematic zone (data not shown).

Statistics and Reproducibility

Experiments were independently repeated three times with similar results.

Data Availability Statement

All RNA-seq data in this study have been deposited in NCBI GEO, with the accession identifier GSE108730.

Code Availability Statement

All code in this study is available upon request.

Extended Data

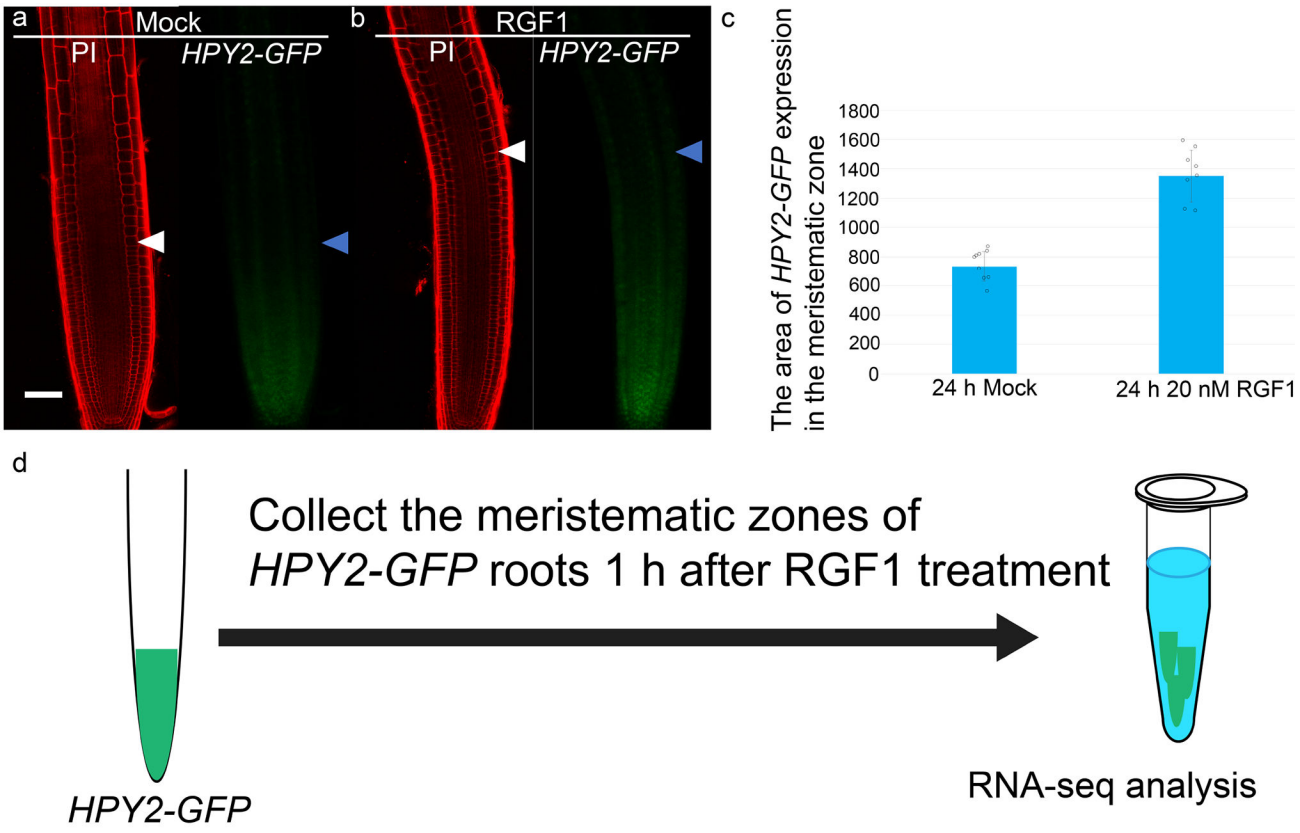

Extended Data Fig. 1. Expression of meristematic zone marker and transcriptome analysis upon RGF1 treatment.

Confocal images of *HPY2-GFP* are shown 24 h after treatment with (a) water (mock) or (b) 20 nM RGF1. Seedlings were grown on MS medium for seven days before treatment. (a and b left) Propidium iodide stained roots; (a and b right) GFP signals. White and blue arrowheads indicate junction between meristematic and elongation zones. Scale bar = 50 μm. (c) Area (μm^2) of *HPY2-GFP* expression is shown. (n = 8 independent roots, p < 2.5E-07). Bar graphs represent mean. Error bars are ± SD. Dots indicate each data point. P values calculated by two-sided Student's t-test. (d) Schematic of RNA extraction following RGF1 treatment.

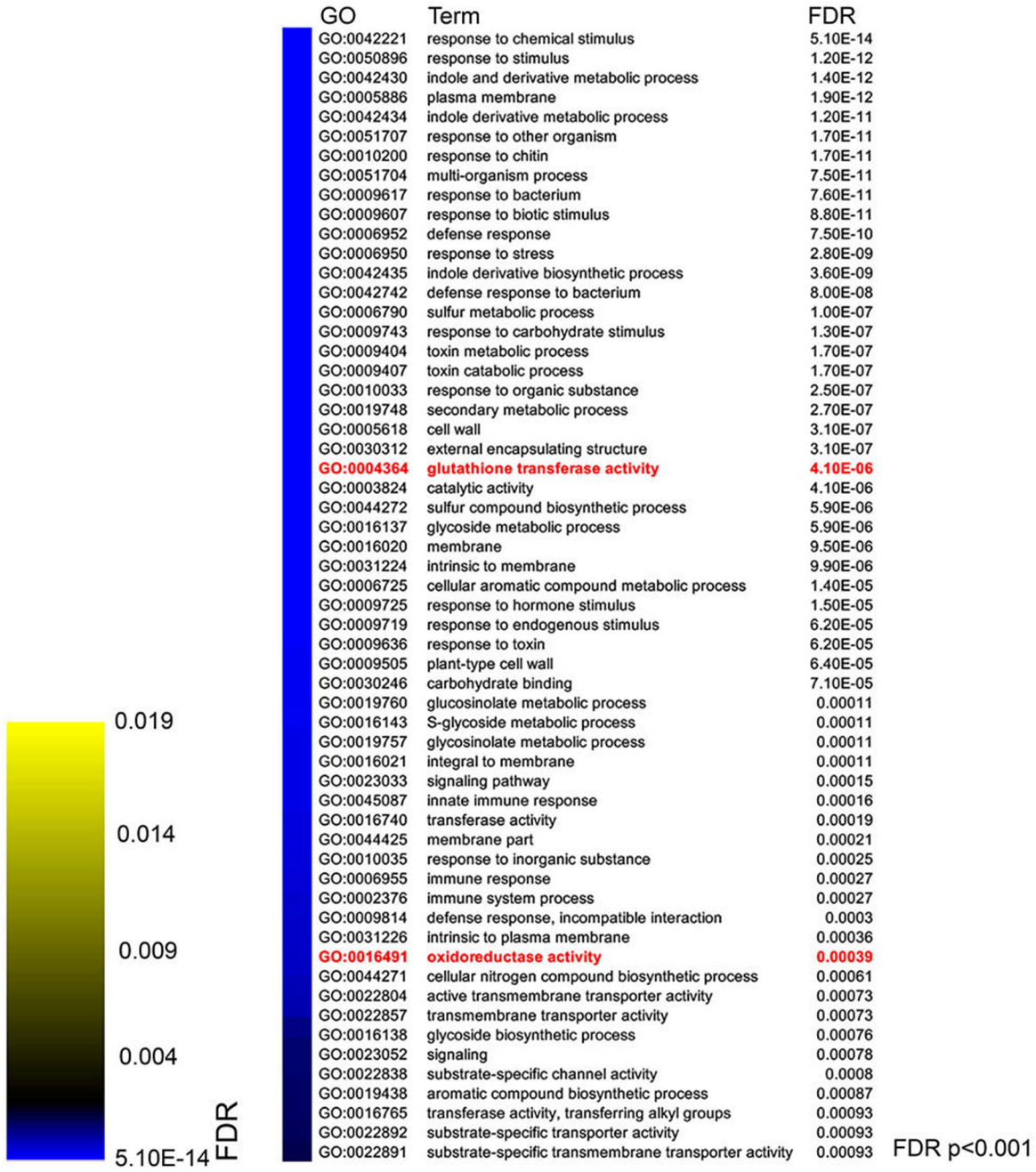

Extended Data Fig. 2. Enriched GO categories upon RGF1 treatment

The highly significant Enriched Gene Ontology (GO) categories within gene lists regulated by RGF1 (False Discovery Rate (FDR)-adjusted p<0.001). “glutathione transferase activity” (FDR-adjusted p= 4.1E-06, red) and “oxidoreductase activity” (FDR-adjusted p=0.00039, red) were highly significantly enriched. See also Extended Data Tables (Enriched GO categories upon RGF1 treatment). The p-value of GO enrichment analysis was based on Fisher’s exact test, with the sample size of all genes in the genome and Benjamini–Yekutieli FDR for multiple testing correction.

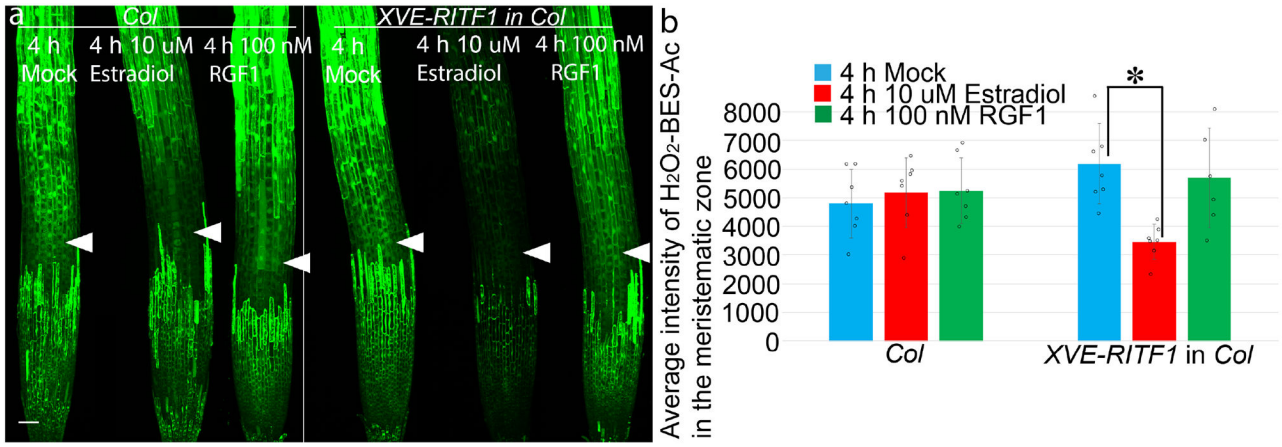

Extended Data Fig. 3. H_2O_2 levels after inducible overexpression of *RITF1* and RGF1 treatment

(a) Confocal images of H_2O_2-BES-Ac stained roots with or without *XVE-RITF1* in wild type 4 h after treatment with water (mock), 10 μM Estradiol, or 100 nM RGF1. (b) Quantification of H_2O_2-BES-Ac intensity in the meristematic zone (n = 6 independent samples, *p < 0.001). Bar graphs represent mean. Error bars are ± SD. Dots indicate each data point. P values calculated by two-sided Student's t-test.

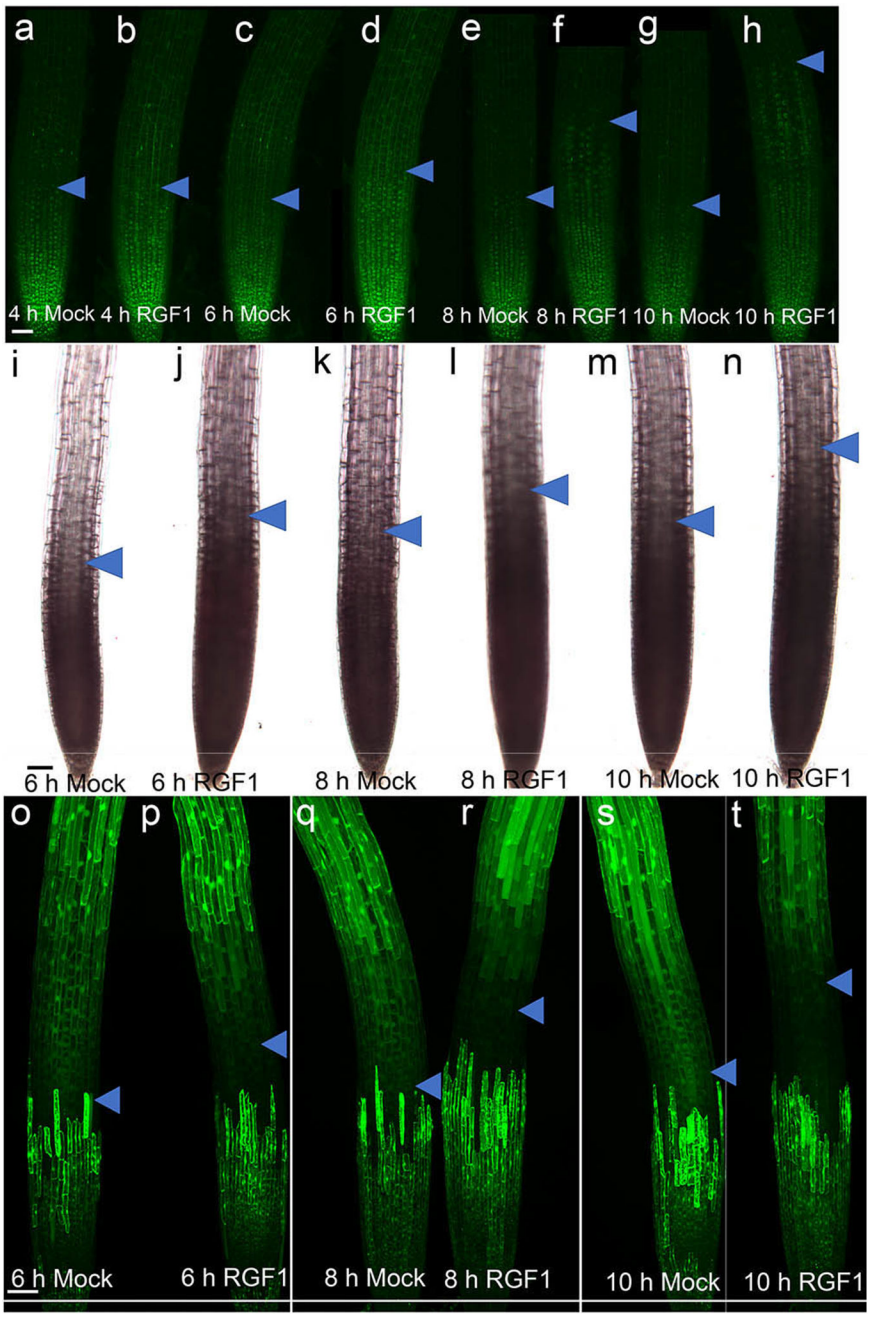

Extended Data Fig. 4. Localization of gPLT2-YFP, NBT, and H_2O_2-BES-Ac staining after RGF1 treatment.

Localization of gPLT2-YFP (a-h), NBT, (i-n) H_2O_2-BES-Ac (o-t), 4 h after treatment with water (mock) (a) or 100 nM RGF1 (b), 6 h after treatment with water (mock) (c, i, and o) or 100 nM RGF1 (d, j, and p), 8 h after treatment with mock (e, k, and q), or 100 nM RGF1 (f, l, and r). 10 h after treatment with mock (g, m, and s) or 100 nM RGF1 (h, n, and t). Blue arrowheads indicate junction between the meristematic and elongation zones. Scale bar = 50 μm. Seedlings were grown on MS agar plates for seven days before treatment. Experiments were independently repeated three times with similar results.

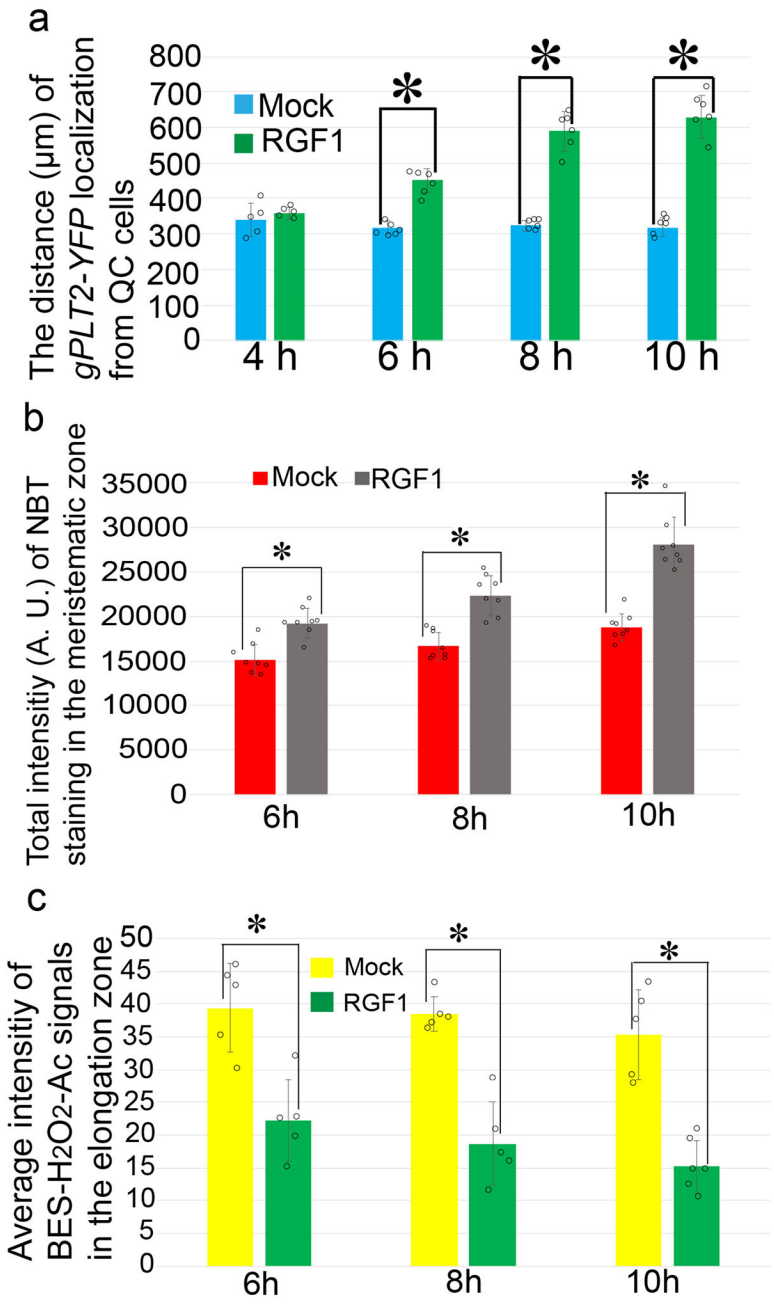

Extended Data Fig. 5. Time course of gPLT2-YFP localization and NBT and H_2O_2-BES-Ac staining

(a) Distance (μm) of gPLT2-YFP localization. (n = 5 independent roots, p < 5.7E-06) (b) Total intensity (arbitrary unit, A. U.) of NBT staining in the meristematic zone. (n = 9 independent roots, p < 0.001) (c) Average intensity of H_2O_2-BES-Ac staining in the elongation zone. (n = 5 independent roots, p < 0.003). Bar graphs represent mean. Error bars are ± SD. Dots indicate each data point. P values calculated by two-sided Student's t-test. Experiments were independently repeated three times with similar results.

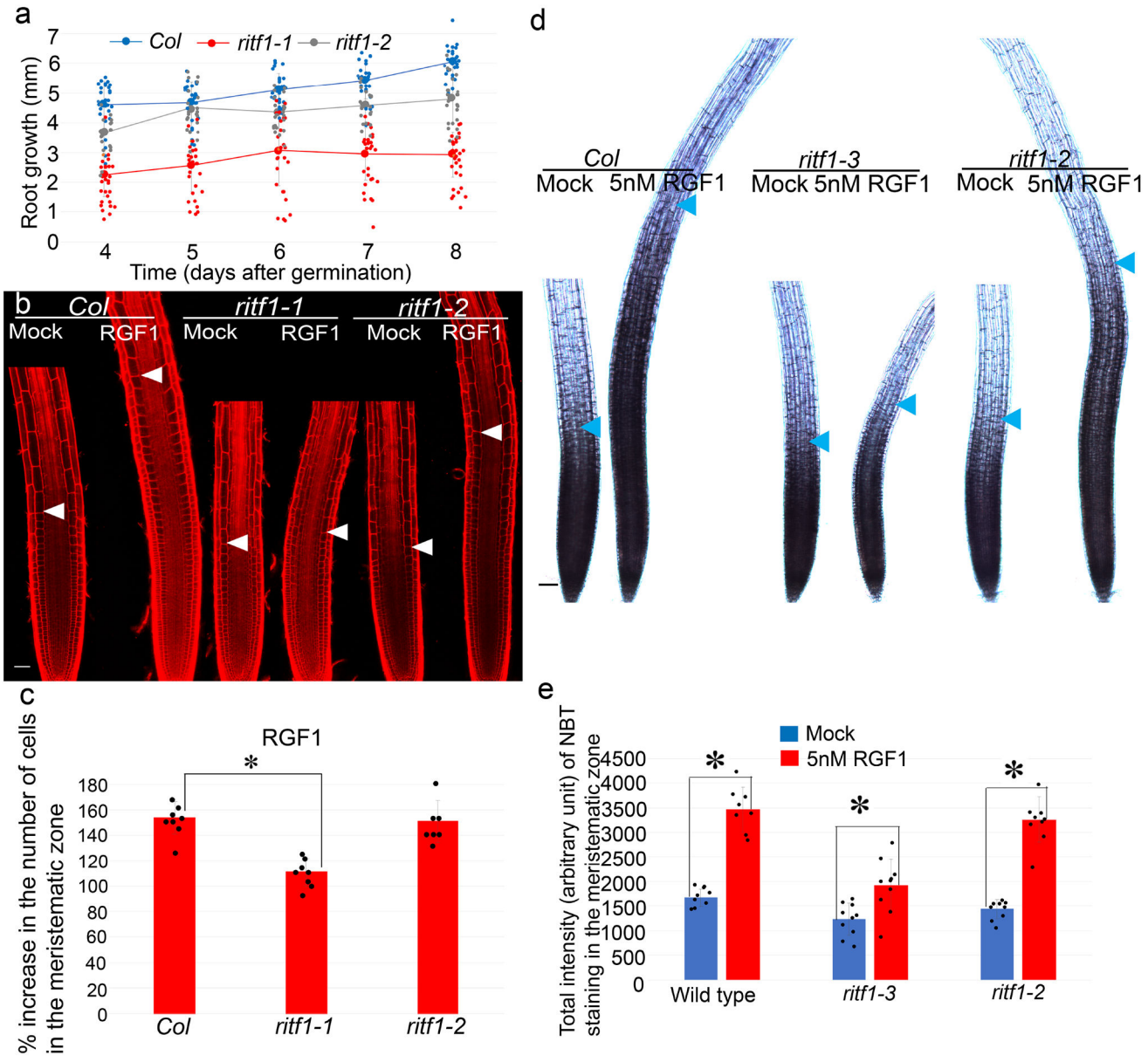

Extended Data Fig. 6. Phenotype of *ritf1*

(a) Root growth (mm) of wild type (Col), *ritf1-1* (CRISPR mutant) and *ritf1-2* (SALK line) from 4 to 8 days after germination. (n = 21 independent roots) (b) Confocal images of roots of *Col*, *ritf1-1* (CRISPR mutant), and *ritf1*-2 (Salk line) stained with PI. (c) Percent increase (100% = number of cells in mock treatment) in the number of cells in the meristematic zone of *Col*, *ritf1-1*, and *ritf1-2* 24 h after mock or 5 nM RGF1 treatment. (n = 7 independent roots, *p < 6.0E-06). (d) Light microscope images of roots of Col, *ritf1-3*, and *ritf1-2* stained with NBT 24 h after 5 nM RGF1 treatment. Scale bar = 50 μm. Blue arrowheads show junction between the meristematic and elongation zones. (e) Quantification of NBT staining intensity (A.U.) in the meristematic zone in wild type, *ritf1-3*, and *ritf1-2* after 5 nM RGF1 treatment. (n = 8 independent roots, *p< 0.003). All scale bars = 50 μm. Blue, and white arrowheads indicate the junction between the meristematic and elongation zones. Bar and

line graphs represent mean. Error bars are ± SD. Dots indicate each data point. P values calculated by two-sided Student's t-test.

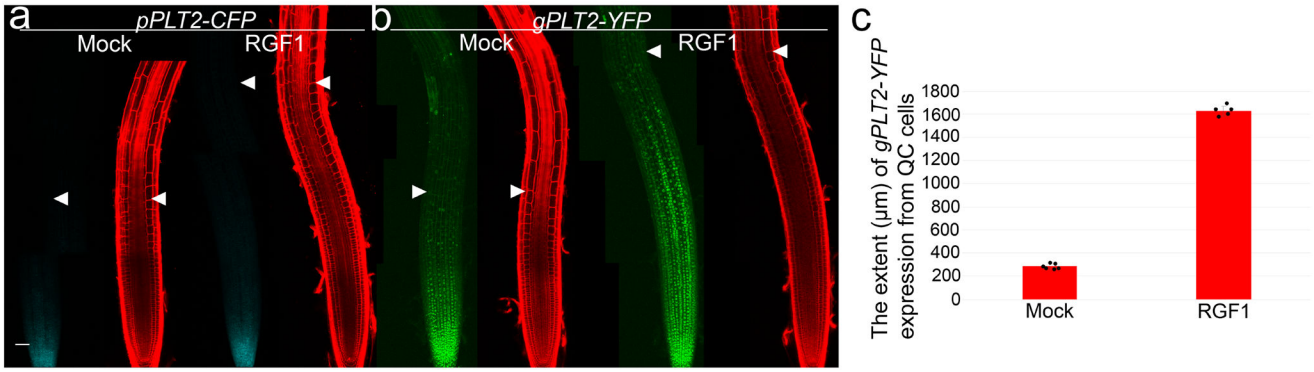

Extended Data Fig. 7. Expression of *pPLT2-CFP* and *gPLT2-YFP* upon RGF1 treatment.

Confocal images of (a) *pPLT2-CFP* and (b) *gPLT2-YFP* 24h after 20 nM RGF1 treatment. PI staining (right images, a and b). Scale bar = 50 μm. Arrow heads show junction between the meristematic and elongation zones. (c). Extent (μm) of expression of *gPLT2-YFP* from QC cells. (n = 5 independent roots, p < 2.5E-13). Bar graphs represent mean. Error bars are ± SD. Dots indicate each data point. P values calculated by two-sided Student's t-test.

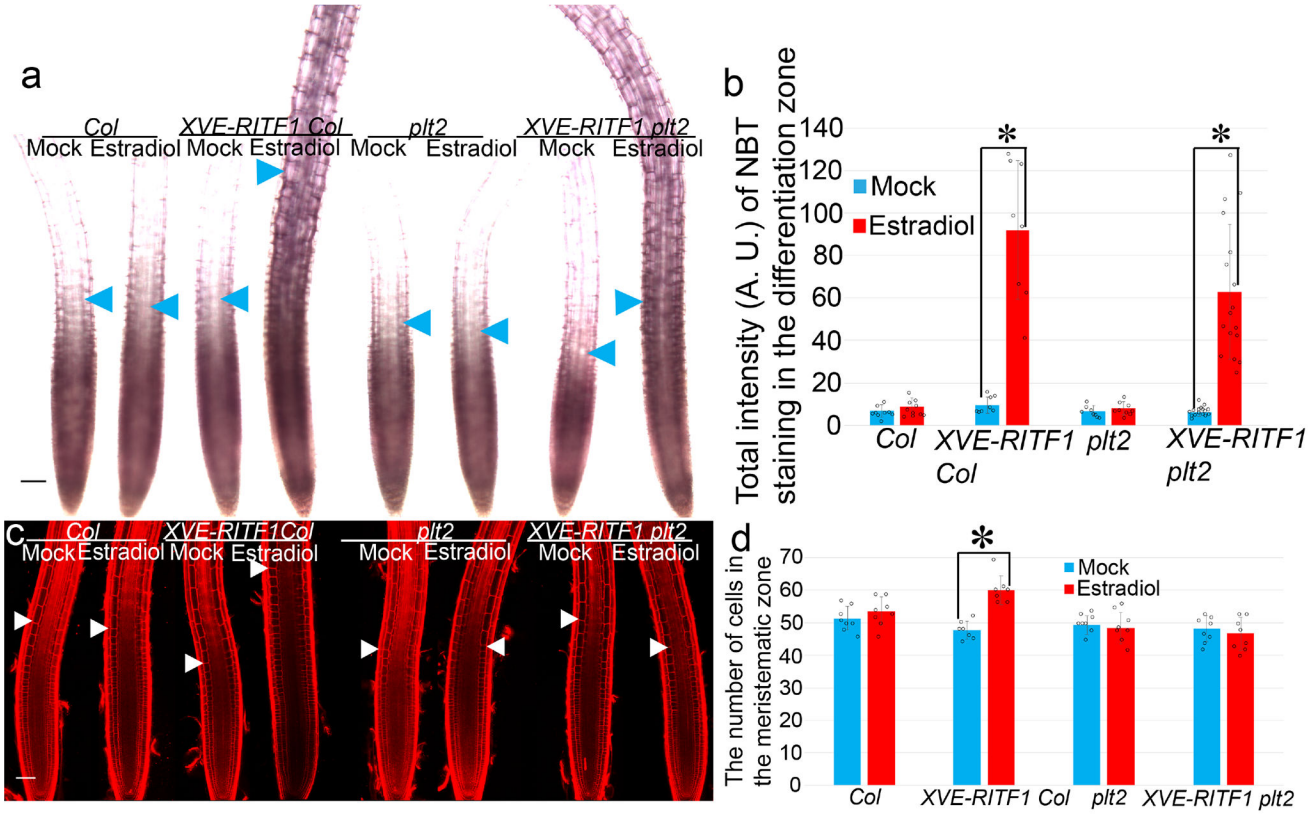

Extended Data Fig. 8. Localization of PLT2 protein after RGF1 and H_2O_2 treatment.

(a-d) Confocal images of gPLT2-YFP 24h after treatment with mock, 20 nM RGF1, 20 nM RGF1 with 500 μM H_2O_2, and 500 μM H_2O_2. Seedlings of *gPLT2-YFP* were grown for seven days on MS agar plates before treatments. Scale bar = 50 μm. Arrow heads show the extent of *gPLT2-YFP* expression. (e) Extent (μm) of PLT2 protein localization as measured from the QC cells. (n = 6, *p < 0.0002). Bar graphs represent mean. Error bars are ± SD. Dots indicate each data point. P values calculated by two-sided Student's t-test.

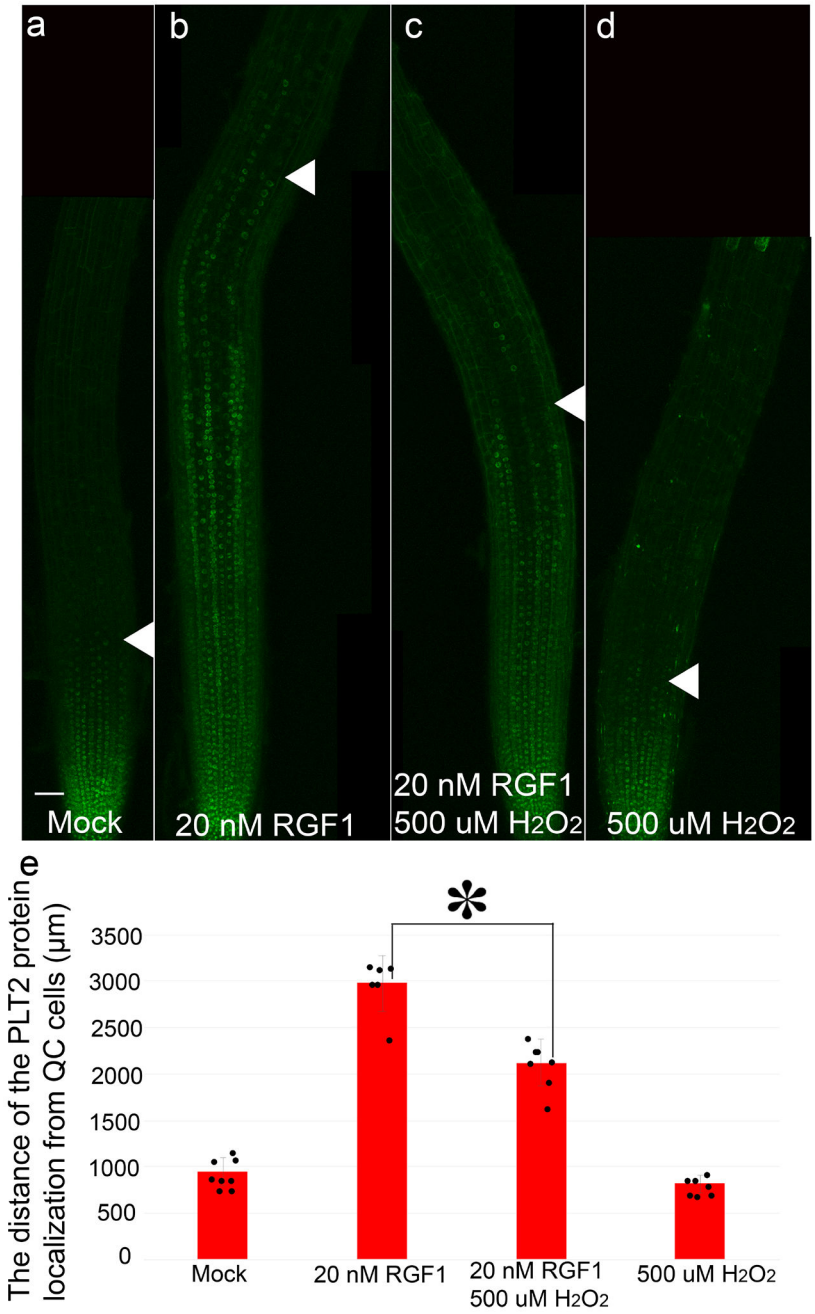

Extended Data Fig. 9. Phenotypes of overexpression of *RITF1* in *plt2*

(a) NBT stained roots with or without *XVE-RITF1* in *Col* and *plt2* 24 h after treatment with mock or 10 μM Estradiol. (b) Quantification of NBT staining intensity in the differentiation zone with or without *XVE-RITF1* in *Col* and *plt2*. (n = 8 independent roots, *p < 5.5E-06). (c) Confocal images of roots with or without *XVE-RITF1* in *Col* and *plt2* 24 h after mock or 10 μM estradiol treatment stained with PI. (d) The number of cells in the meristematic zone with or without *XVE-RITF1* in *Col* and *plt2* 24 h after mock or 10 μM estradiol treatment. (n = 7 independent roots, *p < 4.5E-05). All scale bars = 50 μm. White and blue arrowheads indicate junction between the meristematic and elongation zones. Bar graphs represent

mean. Error bars are ± SD. Dots indicate each data point. P values calculated by two-sided Student’s t-test.

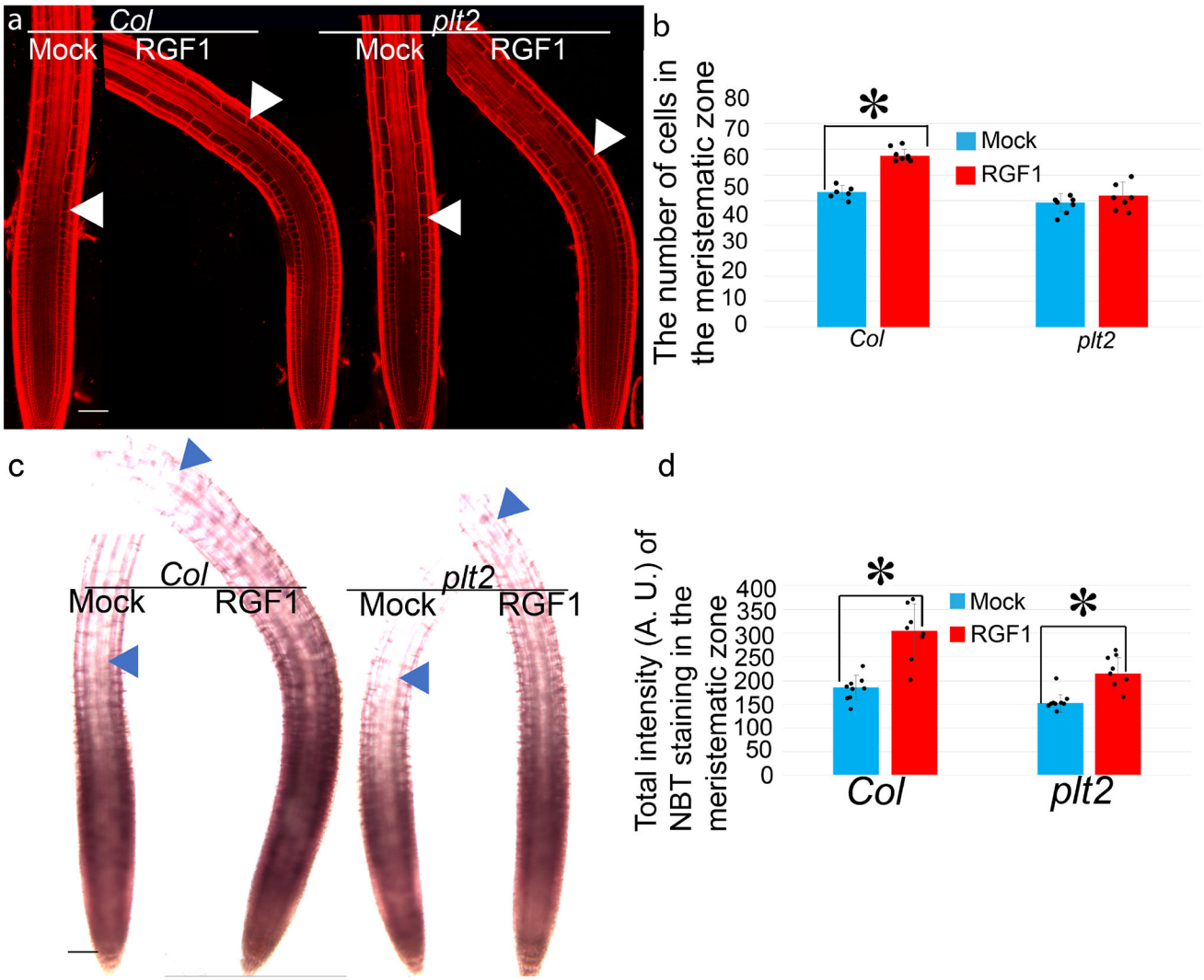

Extended Data Fig. 10. Phenotype of *plt2* upon RGF1 treatment

(a) Confocal images of PI stained roots in wild type (Col) and *plt2* 24 h after 20 nM RGF1 treatment. Scale bar = 50 μm. White arrow heads show junction between the meristematic and elongation zones. (b) Number of cells in the meristematic zone 24 h after 5 nM RGF1 treatment. (n = 8 independent roots, *p < 5E-07). (c) Light microscope images of roots of *Col* and *plt2* stained with NBT. Seedlings were grown on MS agar plates for seven days before mock or 20 nM RGF1 treatment. (d) Total intensity of NBT staining in the differentiation zone of *Col* and *plt2* 24 h after mock or 20 nM RGF1 treatment. (n = 10 independent roots, *p < 0.001). All scale bars = 50 μm. White arrowheads show junction between the meristematic and elongation zones. Bar graphs represent mean. Error bars are ± SD. Dots indicate each data point. P values calculated by two-sided Student's t-test.

Supplementary Material

Refer to Web version on PubMed Central for supplementary material.

Acknowledgments:

We thank I. Taylor, J. Dickinson, E. Pierre-Jerome, K. Lehner, and C. Winter for comments on the manuscript; C. Wilson for help generating overexpression lines; G. Yang for help identifying CRISPR mutants; K. Sugimoto for *HYP2-GFP* seed; Y. Matsubayashi for *rgfr1/2/3* seed; R. Heidstra for *gPLT2-YFP* and *pPLT2-CFP* seed; N-H Chua for the pMDC7 vector; The Duke Genome Sequencing Center for sequencing Illumina libraries; the Plant Tech Core Facility in Agricultural Biotechnology Research Center for generating the CRISPR construct; The Transgenic Plant Laboratory in Academia Sinica for transforming the CRISPR construct into plants. This work was funded by the Howard Hughes Medical Institute and the Gordon and Betty Moore Foundation (through Grant GBMF3405) and from the NIH (MIRA 1R35GM131725) to P.N.B. and by Academia Sinica, Taiwan to M.Y.

References:

1. Dunand C, Crevecoeur M & Penel C Distribution of superoxide and hydrogen peroxide in Arabidopsis root and their influence on root development: possible interaction with peroxidases. New Phytol 174, 332–341, doi:10.1111/j.1469-8137.2007.01995.x (2007). [PubMed: 17388896]
2. Tsukagoshi H, Busch W & Benfey PN Transcriptional regulation of ROS controls transition from proliferation to differentiation in the root. Cell 143, 606–616, doi:10.1016/j.cell.2010.10.020 (2010). [PubMed: 21074051]
3. Matsuzaki Y, Ogawa-Ohnishi M, Mori A & Matsubayashi Y Secreted peptide signals required for maintenance of root stem cell niche in Arabidopsis. Science 329, 1065–1067, doi:10.1126/science.1191132 (2010). [PubMed: 20798316]
4. Whitford R et al. GOLVEN secretory peptides regulate auxin carrier turnover during plant gravitropic responses. Dev Cell 22, 678–685, doi:10.1016/j.devcel.2012.02.002 (2012). [PubMed: 22421050]
5. Meng L, Buchanan BB, Feldman LJ & Luan S CLE-like (CLEL) peptides control the pattern of root growth and lateral root development in Arabidopsis. Proc Natl Acad Sci U S A 109, 1760–1765, doi:10.1073/pnas.1119864109 (2012). [PubMed: 22307643]
6. Ou Y et al. RGF1 INSENSITIVE 1 to 5, a group of LRR receptor-like kinases, are essential for the perception of root meristem growth factor 1 in Arabidopsis thaliana. Cell Res 26, 686–698, doi:10.1038/cr.2016.63 (2016). [PubMed: 27229312]
7. Shinohara H, Mori A, Yasue N, Sumida K & Matsubayashi Y Identification of three LRR-RKs involved in perception of root meristem growth factor in Arabidopsis. Proc Natl Acad Sci U S A 113, 3897–3902, doi:10.1073/pnas.1522639113 (2016). [PubMed: 27001831]
8. Song W et al. Signature motif-guided identification of receptors for peptide hormones essential for root meristem growth. Cell Res 26, 674–685, doi:10.1038/cr.2016.62 (2016). [PubMed: 27229311]
9. Aida M et al. The PLETHORA genes mediate patterning of the Arabidopsis root stem cell niche. Cell 119, 109–120, doi:10.1016/j.cell.2004.09.018 (2004). [PubMed: 15454085]
10. Ishida T et al. SUMO E3 ligase HIGH PLOIDY2 regulates endocycle onset and meristem maintenance in Arabidopsis. Plant Cell 21, 2284–2297, doi:10.1105/tpc.109.068072 (2009). [PubMed: 19666737]
11. Li S, Yamada M, Han X, Ohler U & Benfey PN High-Resolution Expression Map of the Arabidopsis Root Reveals Alternative Splicing and lincRNA Regulation. Dev Cell 39, 508–522, doi:10.1016/j.devcel.2016.10.012 (2016). [PubMed: 27840108]
12. Curtis MD & Grossniklaus U A gateway cloning vector set for high-throughput functional analysis of genes in planta. Plant Physiol 133, 462–469, doi:10.1104/pp.103.027979 (2003). [PubMed: 14555774]
13. Galinha C et al. PLETHORA proteins as dose-dependent master regulators of Arabidopsis root development. Nature 449, 1053–1057, doi:10.1038/nature06206 (2007). [PubMed: 17960244]
14. Licausi F, Ohme-Takagi M & Perata P APETALA2/Ethylene Responsive Factor (AP2/ERF) transcription factors: mediators of stress responses and developmental programs. New Phytol 199, 639–649 (2013). [PubMed: 24010138]
15. Shaikhali J et al. The redox-sensitive transcription factor Rap2.4a controls nuclear expression of 2-Cys peroxiredoxin A and other chloroplast antioxidant enzymes. BMC Plant Biol 8, 48, doi:10.1186/1471-2229-8-48 (2008). [PubMed: 18439303]

16. Waszczak C et al. Sulfenome mining in Arabidopsis thaliana. Proc Natl Acad Sci U S A 111, 11545–11550, doi:10.1073/pnas.1411607111 (2014). [PubMed: 25049418]

17. Dietz KJ, Vogel MO & Viehhauser A AP2/EREBP transcription factors are part of gene regulatory networks and integrate metabolic, hormonal and environmental signals in stress acclimation and retrograde signalling. Protoplasma 245, 3–14, doi:10.1007/s00709-010-0142-8 (2010). [PubMed: 20411284]

18. Licausi F et al. Oxygen sensing in plants is mediated by an N-end rule pathway for protein destabilization. Nature 479, 419–422, doi:10.1038/nature10536 (2011). [PubMed: 22020282]

19. Welsch R, Maass D, Voegel T, Dellapenna D & Beyer P Transcription factor RAP2.2 and its interacting partner SINAT2: stable elements in the carotenogenesis of Arabidopsis leaves. Plant Physiol 145, 1073–1085, doi:10.1104/pp.107.104828 (2007). [PubMed: 17873090]

20. Wang ZP et al. Egg cell-specific promoter-controlled CRISPR/Cas9 efficiently generates homozygous mutants for multiple target genes in Arabidopsis in a single generation. Genome Biol 16, 144, doi:10.1186/s13059-015-0715-0 (2015). [PubMed: 26193878]

21. Maeda H et al. Fluorescent probes for hydrogen peroxide based on a non-oxidative mechanism. Angew Chem Int Ed Engl 43, 2389–2391, doi:10.1002/anie.200452381 (2004). [PubMed: 15114569]

22. Schindelin J et al. Fiji: an open-source platform for biological-image analysis. Nat Methods 9, 676–682, doi:10.1038/nmeth.2019 (2012). [PubMed: 22743772]

23. Zuo J, Niu QW & Chua NH Technical advance: An estrogen receptor-based transactivator XVE mediates highly inducible gene expression in transgenic plants. Plant J 24, 265–273 (2000). [PubMed: 11069700]

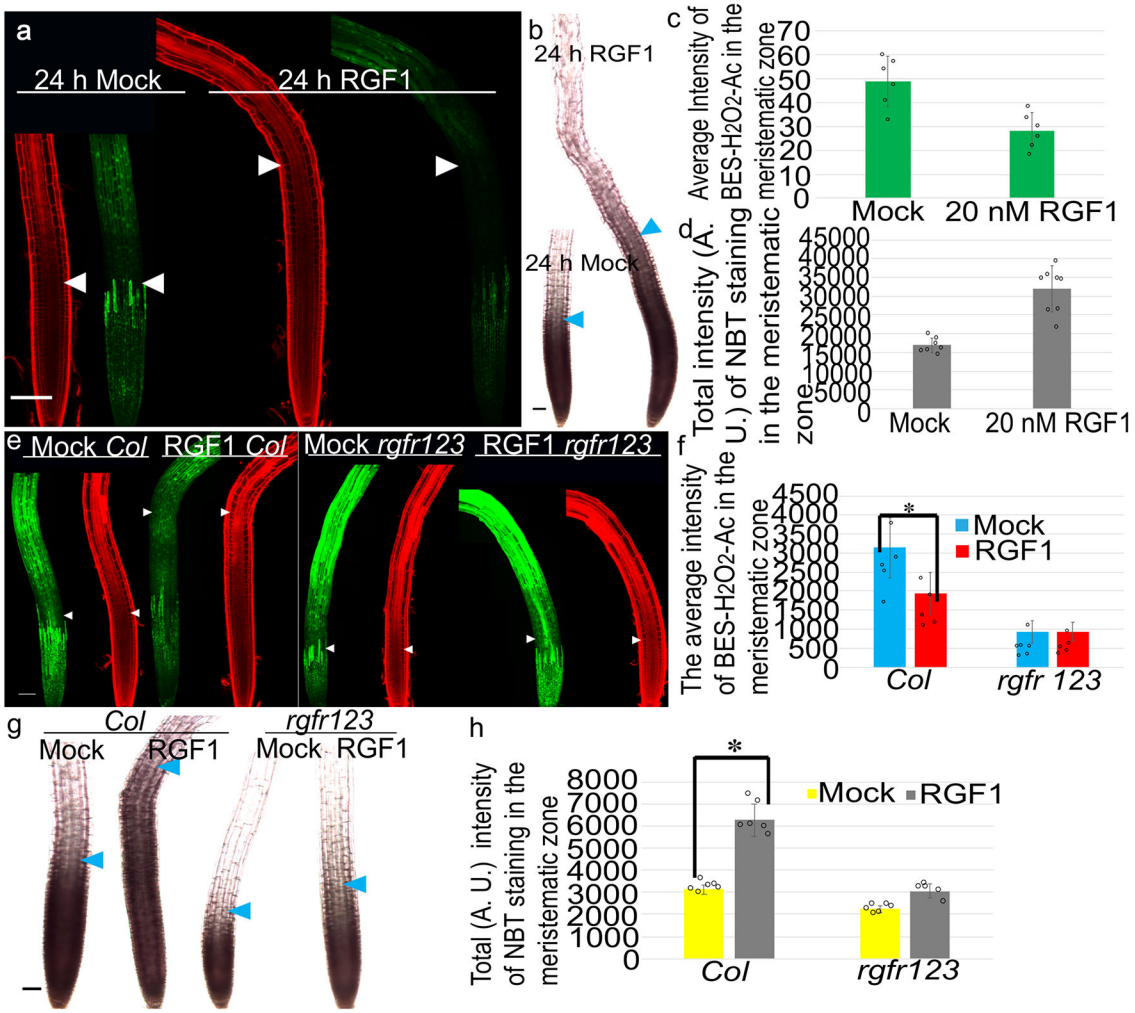

Figure 1. Distribution of ROS levels upon RGF1 treatment.

(a) Confocal images of roots 24 h after treatment with mock and 20 nM RGF1. Propidium iodide (PI) staining (Red), H_2O_2-BES-Ac fluorescence (Green). (b) Roots stained with NBT 24 h after treatment with mock or 20 nM RGF1. (c) Quantification of H_2O_2-BES-Ac intensity in the meristematic zone (n = 6 independent roots, $p < 0.003$). (d) Quantification of NBT staining intensity (arbitrary units (A.U.)) in the meristematic zone (n = 7 independent roots, $p < 0.001$). (e) Confocal images of roots 24 h after treatment with mock or 20 nM RGF1 in wild type (Col-0) or *rgfr 1/2/3*. Staining as in (a). (f) Quantification of H_2O_2-BES-Ac staining intensity in the meristematic zone in wild type and *rgfr 1/2/3* (n = 5 independent roots, *$p < 0.03$). (g) Roots stained with NBT 24 h after treatment with mock or 20 nM RGF1 in wild type or *rgfr 1/2/3*. (h) Quantification of NBT staining intensity (A.U. values) in the meristematic zone in wild type or *rgfr 1/2/3* (n = 5 independent roots, *$p < 0.001$). White and blue arrowheads indicate junction between meristematic and elongation zones. Scale bar = 50 μm. Bar graphs represent mean. Error bars are ± SD. Dots indicate each data point. P values calculated by two-sided Student's t-test.

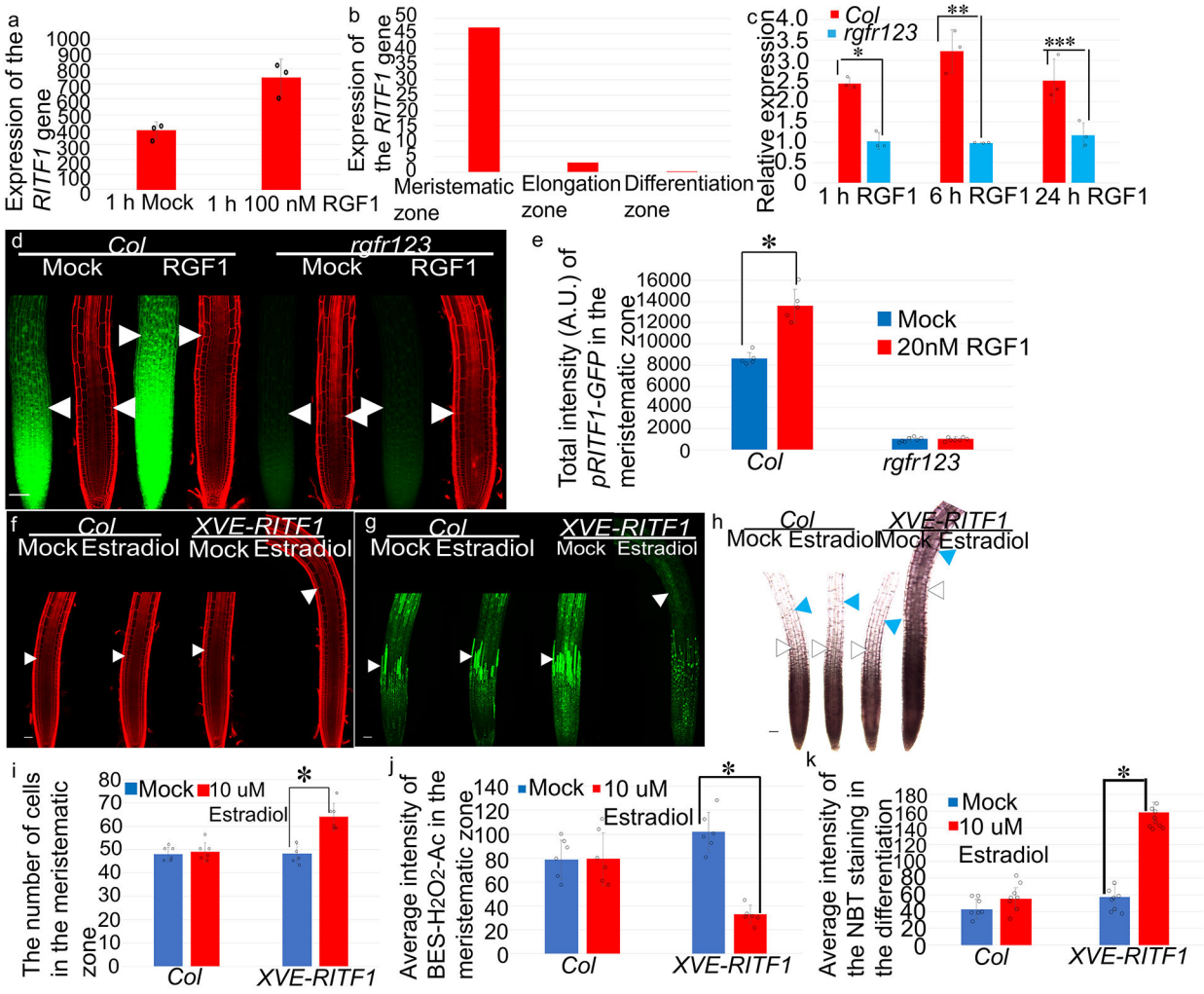

Figure 2. Expression of *RITF1* and phenotype of *RITF1* overexpression line.

(a) Expression of *RITF1* in meristematic zone 1 h after 100 nM RGF1 treatment measured by RNA-seq (CPM, counts per million mapped reads) (n = 3 independent experiments, $p < 0.01$) (b) Expression of *RITF1* in developmental zones measured by RNA-seq (FPKM, Fragments Per Kilobase of transcript per Million mapped reads). (c) Expression of *RITF1* in meristematic zone of wild type and *rgfr1/2/3* upon RGF1 treatment measured by qRT-PCR. (n = 3 independent experiments, *p<0.001, **p<0.002, and ***p<0.02). (d) Confocal images of *pRITF1-GFP* and PI stained root from wild type and the *rgfr1/2/3* after RGF1 treatment. (e) Total intensity (arbitrary unit A.U.) of *pRITF1-GFP* expression in wild type and *rgfr1/2/3* 24 h after RGF1 treatment (n = 5 independent roots, *p < 0.001). Confocal images of roots stained with PI (f) and H_2O_2-BES-Ac (g) in *Col-0* and *XVE-RITF1* in *Col-0* after mock or Estradiol treatment. (h) Light microscope images of NBT stained roots after mock or Estradiol treatment. (i) Number of cells in the meristematic zone in *Col-0* and *XVE-RITF1* after mock or Estradiol treatment. (n = 6 independent roots *p < 0.001). (j) Average intensity of BES-H_2O_2-Ac in differentiation zone after mock or Estradiol treatment (n = 6 independent roots, *p < 0.001). (k) Average intensity of NBT staining in differentiation zone after mock or Estradiol treatments (n = 7 independent roots, *p < 0.001).

Scale bar = 50 μm. White and blue arrowheads indicate junction between meristematic and elongation zones and between elongation and differentiation zones. Bar graphs represent mean. Error bars are ± SD. Dots indicate each data point. P values calculated by two-sided Student's t-test.

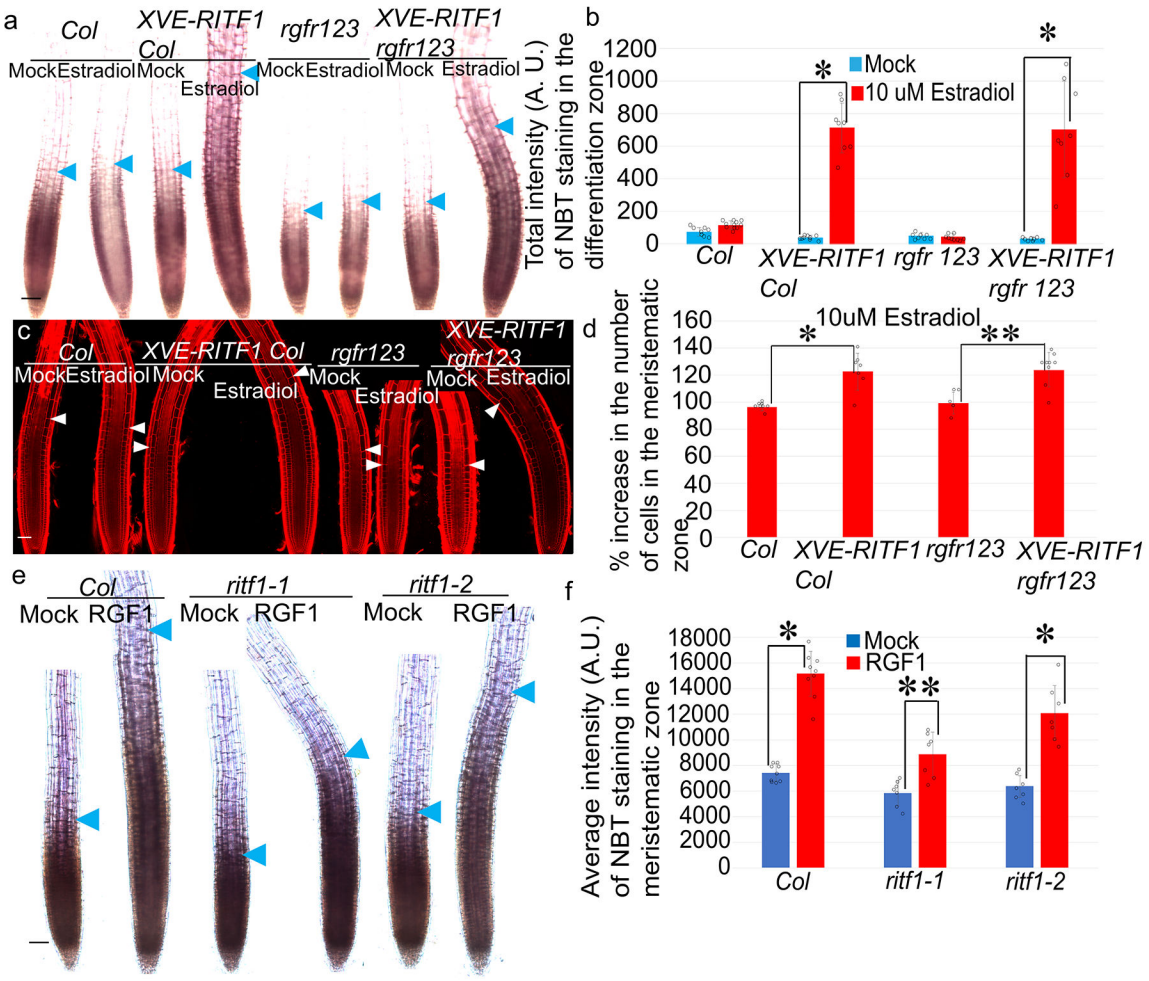

Figure 3. ROS signals and meristem size of *RITF1* overexpression lines in *rgfr1/2/3*

(a) Light microscope images of NBT stained roots with or without *XVE-RITF1* in *Col-0* and *rfgr1/2/3*. (b) Total intensity of NBT staining in differentiation zone with or without *XVE-RITF1* in *Col-0* and *rgfr1/2/3* 24 h after mock or Estradiol treatments. (n = 8 independent roots, *p < 2.0E-05). (c) Confocal images of PI stained roots with or without *XVE-RITF1* in *Col-0* and *rfgr1/2/3*. (d) Percent increase (100% = number of cells in mock treatment) in number of cells in the meristematic zone 24 h after Estradiol treatment compared with mock in *Col-0*, *XVE-RITF1* in *Col-0*, *rgfr1/2/3*, and *XVE-RITF1* in *rgfr1/2/3*. (n = 6 independent roots, *p< 0.0001, **p< 0.001). (e) Light microscope images of roots of *Col-0*, *ritf1-1*, and *ritf1-2* stained with NBT 24h after 5nM RGF1 treatment. Scale bar=50 μm. Blue arrowheads show junction between meristematic and elongation zones. (f) Quantification of NBT staining intensity (A.U.) in meristematic zone in *Col-0*, *ritf1-1*, and *ritf1-2* after 5 nM RGF1 treatment. (n = 7 independent roots, *p < 2.40495E-05, **p < 0.025). Bar graphs represent mean. Error bars are ± SD. Dots indicate each data point. P values calculated by two-sided Student's t-test.

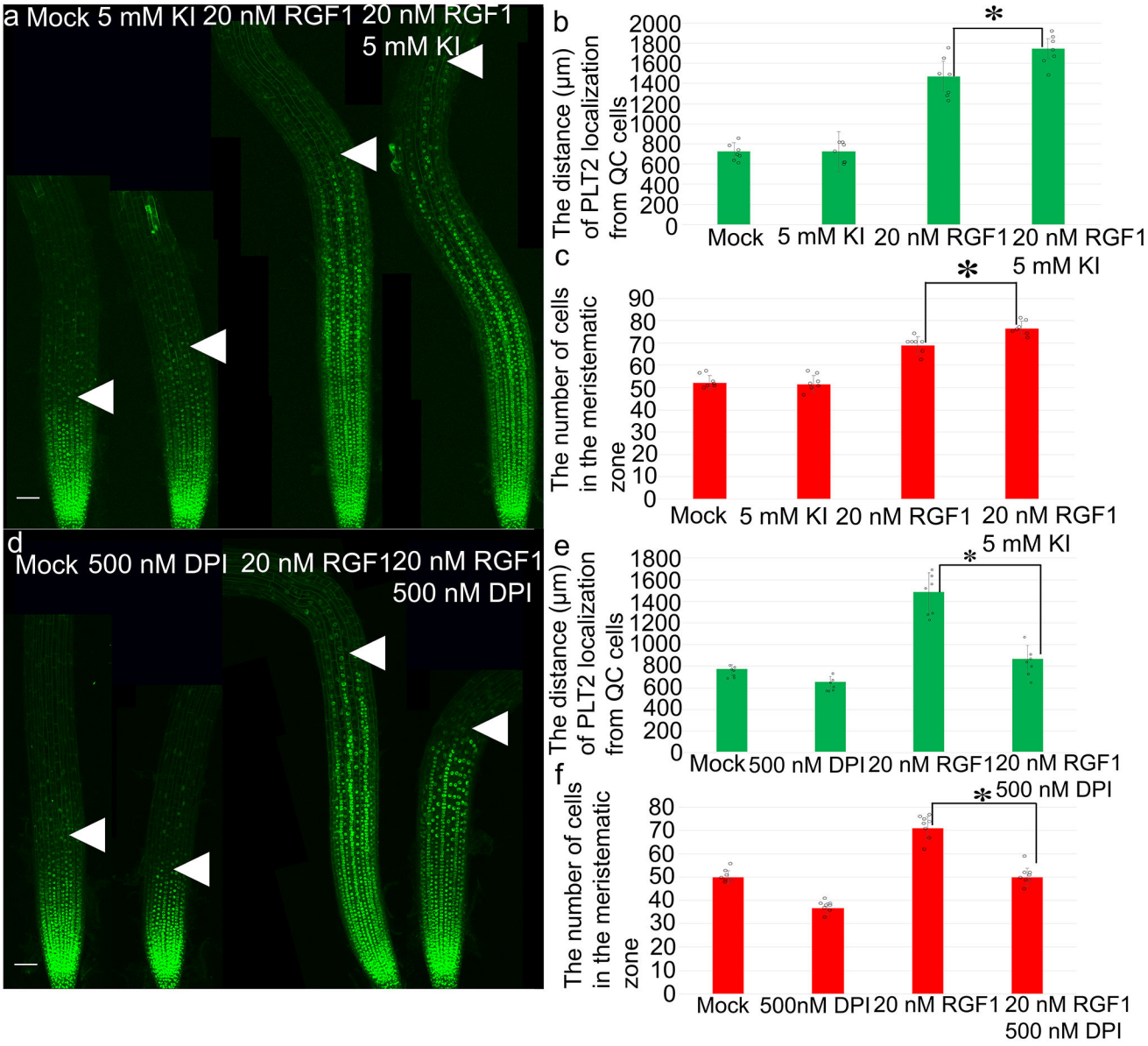

Figure 4. Stability of PLT2 protein upon change in oxidation conditions.

(a and d). Confocal images of gPLT2-YFP 24 h after RGF1, KI (H_2O_2 scavenger), and DPI (NADPH oxidase inhibitor) treatment. (b and e) Localization of gPLT2-YFP upon RGF1 and KI treatment (n = 7 independent roots, *p<0.015) and RGF1 and DPI (n = 7 independent roots, *p<1.5E-05) treatment. (c and f) Meristem size upon RGF1 and KI (n = 7 independent roots, *p<0.002) and RGF1 and DPI (n = 7 independent roots, *p<3.0E-07) treatment. Bar graphs represent mean. Error bars are ± SD. Dots indicate each data point. P values calculated by two-sided Student's t-test.